# Domain-wall interactions. III. High-order phases in the three-state chiral-clock model

Anthony M. Szpilka*
*General Electric Company, Corporate Research and Development, P.O. Box 8, Schenectady, New York 12301*

Michael E. Fisher†
*Baker Laboratory, Cornell University, Ithaca, New York 14853*
(Received 18 May 1987)

A general formalism recently introduced for the study of physical systems exhibiting uniaxial, spatially modulated commensurate phases is applied to the three-state chiral clock ($CC_3$) model in $d>2$ dimensions with arbitrary coordination numbers, $q_0$ in-layer and $q_1$ between layers. Asymptotically exact low-temperature expressions for the domain-wall tension, and for the pair and triplet wall-wall interaction potentials, are calculated explicitly by a transfer-matrix method. The wall interaction potentials determine the phase diagram at low temperatures. The results are compared with those of a similar analysis for the axial next-nearest-neighbor Ising (ANNNI) model, reported in part II: qualitative differences in the phase diagrams directly reflect the different forms of the domain-wall interactions in the two models. The limit of infinite coordination numbers yields the exact low-temperature *mean-field* phase diagram, which is seen to be *qualitatively incorrect* for describing the original, $q_1=2$ $CC_3$ model; the phase diagrams for $q_1\geq 4$ exhibit a *quasitricritical point* on the phase boundary between the modulated and single-domain phases.

## I. INTRODUCTION AND SUMMARY

This is part III of a series of papers on domain-wall interactions in physical systems which may exhibit uniaxial striped phases in which homogeneous domains of an underlying ordered phase are separated by an array of parallel, localized walls at successive separations $l_1, l_2, l_3, \cdots$. The formalism used here and presented in part I of this series,[1] regards the model's exact free-energy density as a sum of domain wall tensions, $\Sigma(T,\mu,\cdots)$, associated with individual walls, plus pair, triplet, quadruplet, and all higher-order many-wall interaction potentials, $W_n(T,\mu,\cdots;\{l_i\})$, $n\geq 2$, which account for the effective forces exerted by the walls on one another. The determination of the $(T,\mu,\cdots)$ phase diagram proceeds in a hierarchical fashion, whereby the simplest stable wall configurations arise from consideration of only the wall tension and the pair interaction $W_2$, while more complicated intervening phases are stabilized successively by the influence of the three-wall and higher-order interactions $W_{(n\geq 3)}$.

In part II of this series,[2] we applied the approach to the *axial next-nearest-neighbor Ising*, or ANNNI model, in which short-range competing couplings are responsible for the appearance of uniaxial striped phases. A transfer-matrix method was applied in II to calculate asymptotically exact low-temperature expressions for the fundamental domain wall interactions, $W_n$, in $d>2$ dimensions. Here we consider another model with short-range competition, the *three-state chiral clock*, or $CC_3$, model, originally introduced by Ostlund[3] and by Huse.[4] Along one special lattice direction (normal to the domain walls), a chiral field breaks the $Z_3$ symmetry of ordinary nearest-neighbor three-state clock couplings in this model, and supplies the competition which, in the ANNNI model, is created by the presence of first- and second-neighbor Ising couplings of opposite sign. Consequently, the phase diagrams of the ANNNI and $CC_3$ models, in the plane of competition parameter versus temperature, have certain resemblances even though there are significant differences which can be attributed directly to the different types of wall interactions in the two models. A brief comparative summary of our results for these two models, together with an outline of the approach described in I, has been published.[5]

Our transfer-matrix calculations extend the $CC_3$ model to arbitrary in-layer and interlayer coordination numbers, $q_0$ and $q_1$. For the simple cubic lattice with $q_1=2$, the only case hitherto considered, it turns out that we can employ the same matrices introduced by Yeomans and Fisher[6,7] to calculate the coefficients in a low-temperature series expansion of the $CC_3$ free energy: the resulting phase diagram which we obtain corroborates their findings. (See Fig. 1 of Ref. 6 and Fig. 3, below.) Upon extending these calculations to arbitrary $q_1\geq 4$, however, we find that qualitative changes ensue in the phase diagram: see Fig. 3 below which summarizes our findings.[5] Specifically, the model now exhibits a *quasitricritical point* at which the transition between the "commensurate," or single-domain, and "incommensurate," or spatially modulated, phases switches from first order to quasicontinuous: a general analysis of this phenomenon was given in I. Insofar as the quasitricritical point persists even in the limit of infinite coordination numbers, where we obtain the the exact *mean-field limit* of the model, it follows that mean-field theory gives a *qualitatively incorrect* picture of the original ($q_1=2$) $CC_3$ phase diagram even at arbitrarily low temperatures. This somewhat surprising result explains a discrepancy recently discovered between the asymptotically exact low-temperature $q_1=2$ phase diagram derived by Yeomans and Fisher,[6,7] and a series expansion of the mean-

 

field $CC_3$ free energy by Siegert and Everts.[8]

The layout of this paper is as follows. Section II introduces necessary notation and summarizes the computational procedure developed in parts I and II of this series. In Sec. III we develop the transfer-matrix calculation of the wall potentials, $W_n$, for the simplest case of interlayer coordination number $q_1=2$. These calculations are extended to arbitrary $q_1>2$ in Sec. IV, and the behavior near the quasitricritical point, which then arises, is examined.

## II. DEFINITIONS AND FORMALISM

The competition among interactions which seems necessary to produce high-order spatially modulated phases is achieved in the ANNNI model by the introduction of an axial *second*-neighbor coupling $J_2$, whose sign is opposite to that of the first-neighbor coupling $J_1$. But one can also create such competition in a model with only nearest-neighbor (NN) couplings, at the expense of replacing the simple binary Ising spins with multistate spins. Perhaps the simplest such models are the $p$-state chiral clock ($CC_p$) models,[3,4] composed of commuting spin variables $n_r$ which take the values $0,1,\ldots,p-1$. It is convenient to visualize these $p$ values of $n_r$ as the $p$ equispaced points around the unit circle that form an angle $(2\pi/p)n_r$ with respect to an arbitrary fixed axis. The spins reside on the sites $\mathbf{r}$ of a $d$-dimensional lattice, in which a special "axial" direction or $z$ axis is singled out. Within every $(d-1)$-dimensional lattice "plane" or "layer" *normal* to this axis, any two spins separated by a nearest-neighbor lattice vector $\boldsymbol{\delta}$ experience the simple "clock" coupling

$$-J_0\cos[(2\pi/p)(n_{\mathbf{r}+\boldsymbol{\delta}}-n_{\mathbf{r}})] .$$

Note that this term can assume $[\frac{1}{2}p]+1$ distinct values, as determined by the $p$ possible distinct values of the cosine's argument. Only for $p=2$ or 3, then, is this intralayer clock coupling equivalent to the fully symmetric Potts model coupling

$$-J_0\delta(n_{\mathbf{r}},n_{\mathbf{r}+\boldsymbol{\delta}}) ,$$

where $\delta(x,y)$ is the Kronecker delta function. In the chiral model, however, spins separated by a nearest-neighbor lattice vector $\boldsymbol{\delta}'$ between *adjacent* layers experience a clock coupling whose mirror symmetry (invariance under spin interchange) is broken by the addition of a *chiral field* $\kappa$. The Hamiltonian is thus taken to be[3]

$$\mathcal{H}=\sum_{\mathbf{r}}\left[-J_0\sum_{\boldsymbol{\delta}}\cos\left[\frac{2\pi}{p}(n_{\mathbf{r}+\boldsymbol{\delta}}-n_{\mathbf{r}})\right]-J_1\sum_{\boldsymbol{\delta}'}\cos\left[\frac{2\pi}{p}(n_{\mathbf{r}+\boldsymbol{\delta}'}-n_{\mathbf{r}}-\kappa)\right]-H_{\mathbf{r}}\cos\left[\frac{2\pi}{p}(n_{\mathbf{r}}-\theta_{\mathbf{r}})\right]\right] , \tag{2.1}$$

where the last term accounts for a possible ordering field $H_{\mathbf{r}}$, acting at site $\mathbf{r}$ at an angle $(2\pi/p)\theta_{\mathbf{r}}$ relative to the spin direction $n_{\mathbf{r}}=0$. Let the coordination numbers within a layer and among adjacent layers be denoted $q_0$ and $q_1$, respectively: for the commonly considered simple cubic lattice, one has $q_0=4$ and $q_1=2$.

In zero field, the chiral-clock Hamiltonian is invariant under the transformations[3,7]

$$\kappa\rightarrow-\kappa,\quad n_{\mathbf{r}}\rightarrow-n_{\mathbf{r}}\ (\mathrm{mod}\,p) \tag{2.2}$$

and

$$\kappa\rightarrow1+\kappa,\quad n_{\mathbf{r}}\rightarrow(n_{\mathbf{r}}+z)\ (\mathrm{mod}\,p) , \tag{2.3}$$

where $z$ denotes the $z$ coordinate of lattice site $\mathbf{r}$ (the lattice constant along the $z$ axis being set to unity). Hence it suffices to study the phase diagram for, e.g., $0\le\kappa\le\frac{1}{2}$ or $\frac{1}{2}\le\kappa\le1$.

It will be assumed throughout that $J_0\ge0$, $J_1\ge0$, and $H_{\mathbf{r}}\equiv0$. Then in the ground state it is clear that, as for the ANNNI model, each layer will be ferromagnetically ordered (all spins taking the same value), so that the ground state can be described by specifying the sequence of these spin values along the $z$ axis. This sequence is readily determined by examination of the second term in (2.1). At $\kappa=0$ (the pure clock model), $\mathcal{H}$ is minimized when

$$\Delta n_{\mathbf{r}}\equiv n_{\mathbf{r}+\boldsymbol{\delta}'}-n_{\mathbf{r}} \tag{2.4}$$

assumes the value 0 (fully ferromagnetic ground state). As $\kappa$ increases toward $\frac{1}{2}$, however, $\Delta n_{\mathbf{r}}=1$ is increasingly favored relative to $\Delta n_{\mathbf{r}}=0$, until at $\kappa=\frac{1}{2}$, the states $\Delta n_{\mathbf{r}}=0$ and $\Delta n_{\mathbf{r}}=1$ are energetically degenerate. For $\frac{1}{2}<\kappa\le1$, the Hamiltonian $\mathcal{H}$ is minimized by $\Delta n_{\mathbf{r}}=1$, so the ground state is the "right-handed helical" sequence

$$\cdots0\,1\,2\cdots(p-1)0\,1\,2\cdots(p-1)0\,1\,2\cdots$$

along the $z$ axis. [Note that this conclusion also follows from the known ferromagnetic ground state for $0\le\kappa<\frac{1}{2}$, by (2.2) and (2.3).] There is thus, as in the ANNNI model, a *multiphase point* of infinite ground-state degeneracy at $\kappa=\frac{1}{2}$: at this point, a ground-state layer sequence may have $\Delta n_{\mathbf{r}}=0$ or 1 for each $\mathbf{r}$ individually. This degeneracy implies a finite zero-temperature entropy per *layer* (of $k_B\ln2$) but still zero entropy per *spin*, in accord with the Third Law of Thermodynamics.

To describe the different possible ground states at the multiphase point $\kappa=\frac{1}{2}$, it is convenient to adopt a notation[6] similar to that used for the ANNNI model (see Sec. II of part II): $\langle j_1j_2\cdots j_n\rangle$ will denote a periodic layer sequence whose fundamental period consists of $j_1$ layers all in the same state $m$ (a "$j_1$ band"), followed by $j_2$ layers all in the state $(m+1)(\mathrm{mod}\,p)$ (a "$j_2$-band"), then a $j_3$-band in the state $(m+2)\ (\mathrm{mod}\,p)$, and so on, concluding with a $j_n$-band. (Note that when $H_r\equiv0$ the value of $m$ does not matter.) Thus, the ferromagnetic sequence is denoted by $\langle\infty\rangle$, and the right-handed helical sequence by $\langle1\rangle$.

For $p=2$, the chiral-clock Hamiltonian (2.1) for any fixed $\kappa$ (and $H_{\mathbf{r}}\equiv0$) is just that of a $d$-dimensional Ising model with uniaxial anisotropy, which exhibits only a simple ferromagnetic-disordered phase transition. [At $\kappa=\frac{1}{2}$, the model decouples into a set of independent

$(d-1)$-dimensional isotropic Ising layers.] To obtain more complicated phases, one must consider $p \geq 3$; most work so far has focused on the case we shall consider, namely, the $(p=3)$-state model. (Some calculations for $p>3$ have been reported by Yeomans.[9,10])

The breaking of the ground-state degeneracy of the multiphase point at low temperatures may be treated along the lines used for the ANNNI model. The low-temperature free-energy series expansion about an arbitrary ground-state configuration, carried out by Fisher and Selke for the ANNNI model and described in II, has also been applied to the $CC_3$ model by Yeomans and Fisher.[6,7] For the $CC_3$ Hamiltonian (2.1), breaking a single "in-layer" ferromagnetic bond is associated with a Boltzmann factor[11]

$$w \equiv e^{-3K_0/2} \quad \text{with } K_i \equiv J_i/k_B T \quad \text{for } i=0,1 \ . \tag{2.5}$$

Hence, the principal small parameter of this free-energy expansion is the total in-layer Boltzmann factor

$$w_0 \equiv w^{q_0} \tag{2.6}$$

associated with "overturning" one spin in a fully ferromagnetic layer. Note that the spin can be flipped to either of *two* other states, but the in-layer pure clock coupling is insensitive to the final state. The axial *chiral* clock coupling *is* sensitive to the flipped spin's final state, however, so the Boltzmann factors associated with changes in axial NN bonds can be expressed[7] in terms of two parameters, $y$ and $\theta$, defined by the weights

$$(00\rightarrow 01)=(11\rightarrow 12)=(22\rightarrow 20)=\exp\left\{K_1\left[\cos\left[\frac{2\pi}{3}(1-\kappa)\right]-\cos\left[\frac{2\pi}{3}\kappa\right]\right]\right\}\equiv y^{\theta} \ , \tag{2.7}$$

$$(00\rightarrow 02)=(11\rightarrow 10)=(22\rightarrow 21)=\exp\left\{K_1\left[\cos\left[\frac{2\pi}{3}(2-\kappa)\right]-\cos\left[\frac{2\pi}{3}\kappa\right]\right]\right\}\equiv y \ . \tag{2.8}$$

Thence one has the Boltzmann factor

$$(01\rightarrow 02)=(12\rightarrow 10)=(20\rightarrow 21)=y^{1-\theta} \ , \tag{2.9}$$

since the reverse transitions [like $(01\rightarrow 00)$] are associated with the reciprocal Boltzmann factors. From the $CC_3$ Hamiltonian (2.1), one can relate $y$ and $\theta$ to $w$ and $\kappa$: for this purpose, it is convenient to define a parameter $\delta$ which measures displacement from the multiphase point $\kappa=\frac{1}{2}$ according to

$$\delta \equiv \frac{\cos(2\pi/3)(1-\kappa)}{\cos(2\pi/3)\kappa}-1$$

$$\approx \frac{4\pi}{\sqrt{3}}(\kappa-\tfrac{1}{2}) \quad \text{as } \kappa\rightarrow\tfrac{1}{2} \ . \tag{2.10}$$

One then finds

$$\theta=-\frac{\delta}{\delta+3} \ , \tag{2.11}$$

$$y=w^{J_1/J_0(1-\theta+\theta^2)^{1/2}}=w^{(J_1/J_0)[1-\delta/6+O(\delta^2)]} \ . \tag{2.12}$$

The first step of the series expansion, which considers only a single flipped spin, indicates a wedge of $\langle 2\rangle$ phase in the $(\kappa,T)$ plane, of width $\Delta\kappa=O(K_1^{-1}w_0)$ at fixed small $T$, springing from the multiphase point and separating $\langle\infty\rangle$ from $\langle 1\rangle$. By virtue of the symmetries (2.2) and (2.3), the $\langle\infty\rangle$:$\langle 2\rangle$ and $\langle 2\rangle$:$\langle 1\rangle$ pseudoboundaries are mirror images of each other in the line $\kappa=\frac{1}{2}$; we shall confine our attention to the $\langle 2\rangle$:$\langle 1\rangle$ pseudoboundary, on which $K_1\delta$ assumes the value[7,11]

$$K_1\delta_1^{(1)}(T)\equiv(8/q_1)(1-y^{q_1/2})^2 w_0 \ . \tag{2.13}$$

On this pseudoboundary, *all layer sequences composed of* 1 *and* 2 *bands only* have the same free energy through order $w_0$. Further terms of the series, of order $w_0^2$ and higher, are needed to resolve which of these sequences actually appear as stable phases between $\langle 2\rangle$ and $\langle 1\rangle$. This $\langle 2\rangle$:$\langle 1\rangle$ pseudoboundary is therefore precisely analogous to the $\langle 3\rangle$:$\langle 2\rangle$ pseudoboundary of the ANNNI model: as in II, one may now characterize all phases that may appear on the $\langle 2\rangle$:$\langle 1\rangle$ pseudoboundary as composed of $\langle 2\rangle$-phase *domains* separated by 1-band *walls*, where a domain of width $k$ is comprised of $k$ adjacent 2 bands, and a wall consists of a single 1 band. Of course, no reason has so far been given for preferring this description of the possible phases to the alternative which regards them as composed of $\langle 1\rangle$-*phase* domains separated by 2-*band* walls: our choice of convention is guided by the results of the complete Yeomans-Fisher expansion,[7] which indicated that the phases interpolating between $\langle 2\rangle$ and $\langle 1\rangle$ are of the form $\langle 12^k\rangle$, in which 1 bands do indeed occur only singly as "walls." It is important to note, however, that our identification of domains and walls at this point is purely arbitrary and will not influence or restrict the set of phases that we subsequently establish as being stable. In particular, for the case of arbitrary interlayer coordination number $q_1>2$ we shall explicitly demonstrate, in Sec. IV B, the stability of phases more complicated than just the "simple periodic" $\langle 12^k\rangle$ phases, and, in Sec. IV C, we shall find it convenient to adopt the alternative convention of $\langle 1\rangle$-phase domains separated by 2-band walls in order to resolve part of the phase diagram more fully.

To proceed with the refinement of the phase diagram according to the formalism of I, we shall find it computationally convenient, as in II, to introduce the reduced free-energy density

$$f \equiv F_N/Nk_B T \ , \tag{2.14}$$

where $F_N$ is the total free energy of a lattice of $N$ sites, and the reduced domain wall tension and wall interactions, namely,

$$\sigma(T,\kappa)=\Sigma(T,\kappa)/k_BT\ ,$$
$$\overline{W}_n(T,\kappa;l_1,\ldots,l_{n-1})=W_n(T,\kappa;l_1,\ldots,l_{n-1})/k_BT. \tag{2.15}$$

Then the reduced free-energy density may be written exactly in terms of the background free-energy density $f_0$ of the pure $\langle 2\rangle$ phase and the reduced $n$-wall interactions $\overline{W}_n$ among the 1-band walls, as

$$f(T,\kappa;\{l_i\})\equiv f_0(T,\kappa)+\Delta f(T,\kappa;\{l_i\})\ , \tag{2.16}$$

with the basic decomposition

$$\Delta f(T,\kappa;\{l_i\})\equiv \lim_{L,\mathcal{N}\to\infty}\frac{1}{L}\sum_{i=1}^{\mathcal{N}}\left[\sigma(T,\kappa)+\sum_{n=2}^{\infty}\overline{W}_n(T,\kappa;l_i,l_{i+1},\ldots,l_{i+n-2})\right]$$
$$=\lim_{L,\mathcal{N}\to\infty}\frac{1}{L}\left[\mathcal{N}\sigma+\sum_{i=1}^{\mathcal{N}}[\overline{W}_2(l_i)+\overline{W}_3(l_i,l_{i+1})+\cdots]\right]\ . \tag{2.17}$$

Here $\mathcal{N}$ denotes the number of walls in a system of $L$ layers, and the $l_i$ denote the axial distances between successive walls: specifically, if there are $k_i$ 2 bands between the $i$th and $(i+1)$th 1-band walls, then those two walls are $l_i=2k_i+1$ lattice layers apart (with $l_i\geq 1$). Notice that we must allow for the possibility that two walls may be separated by zero 2 bands in order to retain full generality.

The wall interaction potentials $\overline{W}_n$ in (2.17) may be related to the "standard structural coefficients" of the Yeomans-Fisher free-energy expansion[6,7] in precisely the same manner as was done for the ANNNI model in Secs. II B and II C of II, if every mention of a "3 band" there is replaced by "1 band." Therefore, in the remainder of this section, we only summarize the correspondence, referring the reader to II for more detailed discussion and proofs. Following Yeomans and Fisher,[6,7,12] we may write the reduced free-energy density as

$$f(\{\rho_\nu\};w,y,\delta)\equiv a_0(w,y;\delta)+\sum_\nu a_\nu(w,y;\delta)\rho_\nu\ , \tag{2.18}$$

where the $\rho_\nu$ are variables which denote the number of occurrences per layer of the layer sequence $\nu$ in the ground-state configuration about which the series expansion is being done. For example, the configuration $\langle 1212^2\rangle$ of period eight layers has $\rho_1=\frac{2}{8}=\frac{1}{4}$, $\rho_2=\frac{3}{8}$, $\rho_{12}=\frac{2}{8}=\frac{1}{4}$, $\rho_{121}=\frac{1}{8}$, etc. These $\rho_\nu$ are not all independent variables, but satisfy various linear relations, analogous to Eq. (2.16) of II; the sum in (2.18) extends only over a *linearly independent* or "standard" subset of all possible layer sequences $\nu$ constructed according to the following convention.[12]

*The standard sequence of length $m+2$ bands built from an inner core sequence $\nu$ of length $m$ bands is* $1\nu 1$.

If we introduce the convenient abbreviation

$$a_\nu\equiv(\nu) \tag{2.19}$$

for the standard structural coefficients in (2.18), the reduced wall interactions $\overline{W}_n$ are then directly given by

$$\sigma(T,\kappa)=(1)\ , \tag{2.20}$$
$$\overline{W}_2(T,\kappa;l)=(12^k1)\quad(l=2k+1)\ , \tag{2.21}$$

and, for general $n\geq 3$,

$$\overline{W}_n(l_1,l_2,\ldots,l_{n-1})=(12^{k_1}12^{k_2}\cdots 12^{k_{n-1}}1)\ , \tag{2.22}$$

with $l_i=2k_i+1$. The coefficient $a_1\equiv(1)$ in (2.20) has a nonzero value even in the lowest order (one flipped spin) of the Yeomans-Fisher expansion, which is[7]

$$\sigma(T,\kappa)=a_1(T,\kappa)=-\tfrac{1}{8}q_1K_1[\delta-\delta_1^{(1)}(T)]+O(w_0^2)\ , \tag{2.23}$$

where $K_1\delta_1^{(1)}(T)$ denotes the location of the $\langle 2\rangle$:$\langle 1\rangle$ pseudoboundary as given by (2.13). Thus, the wall tension $\sigma$ vanishes on this pseudoboundary, in accord with the generic behavior discussed in I and the corresponding result for the ANNNI model in Eq. (2.21) of II.

The leading term of the higher-order coefficient $(12^k1)=\overline{W}_2(2k+1)$ is determined by summing the total Boltzmann factors of all the lowest-order excited states of the lattice whose lattice *counts* involve a nonzero value of $\rho_{12^k1}$. Those states are axial *chains* of flipped spins, linked to one another by the coupling $J_1$ and extending across or "spanning" a layer sequence at least as long as $12^k1$. An example is

$$|\hat{s}\,|\underbrace{\hat{s}\hat{s}\,|\hat{s}\hat{s}\,|\hat{s}\hat{s}\,|\hat{s}\hat{s}\,|\cdots|\hat{s}\hat{s}}_{k\ 2\text{-bands}}|\hat{s}\,|\ , \tag{2.24}$$

where each $s$ denotes an entire ferromagnetically ordered layer, a string of adjacent $s$'s indicates a stack of layers all in the same spin state, vertical bars denote band edges, and the circumflex, $\hat{s}$, marks a single overturned spin within the layer. The in-layer Boltzmann factor of an excited state like (2.24) is $w_0^{2k+2}$; consequently, $(12^k1)=O(w_0^{2k+2})$. At this leading order, chains spanning the other three possible (*nonstandard*) layer sequences $1\nu'2$, $2\nu'1$, and $2\nu'2$ (where $\nu'\equiv 2^k$) *also* contribute to $(12^k1)$. The signs to be associated with these contributions are given by:[2]

*Rule 1:* The sequences $2\nu'2$ and $1\nu'1$ contribute negatively to $a_{12^k1}\equiv(12^k1)$, but $2\nu'1$ and $1\nu'2$ contribute positively.

Further contributions at leading order come from all possible axial *decompositions* of any of these chains, through the excluded volume effect: thus, for example,

the excited state consisting of the two *disconnected* segments $|\hat{s}\,|\,\hat{s}\hat{s}\,|$ and $|\hat{s}\hat{s}\,|\,\hat{s}\,|$ contributes to $(12^2 1)$. The signs to be attached to these disconnected configurations are given by:[2]

*Rule 2:* A decomposition into $p$ segments of one of the sequences listed in Rule 1 contributes to $(12^k 1)$ with a sign of $(-1)^{p-1}$.

In summary, then (refer to Sec. III A of part II for a more complete discussion), one obtains the leading term of $(12^k 1)$ [and similarly for the higher-order coefficients of (2.22)] by summing the total Boltzmann factors of all chains of $2k+2$ flipped spins spanning the sequences governed by Rules 1 and 2. This summation, for the simplest case of axial coordination number $q_1=2$, was performed by Yeomans and Fisher using a transfer-matrix method,[7] which we shall describe in Sec. III A; the effect of corrections to these lowest-order expressions will be discussed in Sec. III B. In this way, $\overline{W}_2$ and $\overline{W}_3$ are obtained explicitly, and the resulting phase diagram is deduced. In Sec. IV, we generalize this method to arbitrary $q_1$, and investigate the qualitative changes which result.

## III. THE DOMAIN-WALL POTENTIALS AND THE PHASE DIAGRAM

### A. Lowest-order transfer-matrix results

In order to refine the $(\kappa,T)$ phase diagram within the crossover regime of width $O(w_0^2)$ about the $\langle 2\rangle$:$\langle 1\rangle$ pseudoboundary (2.13), one must, according to Sec. IV of part I, calculate the domain-wall interactions

$$\overline{W}_2(l)=(12^k1)\quad (l=2k+1)\,, \tag{3.1}$$

$$\overline{W}_3(l,l)=(12^k12^k1)\,, \tag{3.2}$$

and so on, where we have recalled the equivalences to the standard structural coefficients $(\nu)\equiv a_\nu$ from (2.21) and (2.22). Consider first the calculation of the coefficient $(12^k1)$. To compute the Boltzmann factor of one of the chains mentioned in Rules 1 and 2, imagine constructing the chain by successively adding on flipped spins to its *left* end. We choose to add bands on the left, as in II (but opposite to the ordering adopted by Yeomans and Fisher[7]), in order to obtain a closer correspondence with standard matrix notation: for the same reason we shall count bands $m=1,2,\ldots$ starting on the *right*. Each newly added flipped spin (call it $\hat{s}_m$) carries a Boltzmann factor $w_0\equiv w^{q_0}$ to account for the broken in-layer bonds, and, additionally, it interacts with its (flipped) axial nearest neighbor to the right, $\hat{s}_{m-1}$. Throughout this section we assume the simplest case of axial coordination number $q_1=2$: there is then only *one* axial nearest neighbor on each side of $s_m$. Now, in their unflipped states, $s_m$ and $s_{m-1}$ might be either in the same band (i.e., $s_m s_{m-1}$), or separated by a band edge $(s_m\,|\,s_{m-1})$. In the former case, the *un*flipped spins $s_m$ and $s_{m-1}$ are both in the same state (which may be taken to be 0 without loss of generality), but the flipped spins $\hat{s}_m$ and $\hat{s}_{m-1}$ can then *independently* be in *either* state 1 or state 2. To account for all four possibilities, it is convenient to write down a $2\times2$ matrix $\mathbf{B}'$ whose $(i,j)$th entry is the Boltzmann factor of the bond $\hat{s}_m\hat{s}_{m-1}$ relative to the bond $s_m s_{m-1}$, when

$$\hat{s}_m=(s_m+i)\ (\mathrm{mod}\,3),\quad \hat{s}_{m-1}=(s_{m-1}+j)\ (\mathrm{mod}\,3)\,, \tag{3.3}$$

for $i,j=1,2$. Using the Boltzmann factors defined in (2.7)–(2.9), one can then write the transfer operator associated with adding $\hat{s}_m$ to the chain of flipped spins as

$$\tilde{\mathbf{V}}(\hat{s}_m\hat{s}_{m-1})\equiv w_0\mathbf{B}'=w_0\begin{bmatrix}1 & y^\theta\\ y & 1\end{bmatrix}. \tag{3.4}$$

Similarly, for the second case mentioned above, where $s_m$ and $s_{m-1}$ are separated by a band edge, say, $(s_m\,|\,s_{m-1})=(0\,|\,1)$, one can have $\hat{s}_m=1$ or 2 and $\hat{s}_{m-1}=2$ or 0. Again, the four possibilities are conveniently recorded in a $2\times2$ matrix $\mathbf{C}'$, with entries defined as in (3.3), so that the transfer operator for this case is

$$\tilde{\mathbf{V}}(\hat{s}_m\,|\,\hat{s}_{m-1})\equiv w_0\mathbf{C}'=w_0\begin{bmatrix}1 & y^{1-\theta}\\ y^{-\theta} & 1\end{bmatrix}. \tag{3.5}$$

The partial partition function (i.e., sum of total Boltzmann factors) of a chain like $\hat{s}\,|\,\hat{s}\hat{s}\,|\,\hat{s}\hat{s}$ then corresponds to the product $w_0^5\mathbf{C}'\mathbf{B}'\mathbf{C}'\mathbf{B}'$, where the definition of matrix multiplication ensures that both possible states of each flipped spin are properly summed over. This matrix product must be left-multiplied by a row vector accounting for the broken axial bond before the leftmost flipped spin of the chain, and right-multiplied by a column vector for the bond after the rightmost flipped spin. The appropriate vectors, which depend on whether these end bonds lie within a band or across a band edge, can readily be deduced from (2.7)–(2.9) as

$$s\hat{s}\colon \mathbf{b}_0^\dagger=[y^\theta,y],\quad s\,|\,\hat{s}\colon \mathbf{c}_0^\dagger=[y^{1-\theta},\,y^{-\theta}]\,, \tag{3.6}$$

and

$$\hat{s}s\colon \mathbf{b}_1=\begin{bmatrix}y\\ y^\theta\end{bmatrix},\quad \hat{s}\,|\,s\colon \mathbf{c}_1=\begin{bmatrix}y^{-\theta}\\ y^{1-\theta}\end{bmatrix}. \tag{3.7}$$

One can, therefore, finally write the partial partition function of a chain, summed over all possible final values of its flipped spins, as, for example,

$$\cdots s\hat{s}\,|\,\hat{s}\hat{s}\,|\,\hat{s}\hat{s}\,|\,s\cdots=\mathbf{b}_0\mathbf{C}'\mathbf{B}'\mathbf{C}'\mathbf{B}'\mathbf{c}_1 w_0^5\,. \tag{3.8}$$

So far, however, this transfer matrix notation applies only to *fully connected* chains. According to Rule 2 of Sec. II, one also needs the Boltzmann factors for all possible *decompositions* of such chains. A decomposition can occur between any two flipped spins of the chain, and carries an extra factor of $-1$. Suppose the chain is separated between two flipped spins labeled $\hat{s}_m$ and $\hat{s}_{m-1}$, which, for purposes of illustration, will be assumed to be in the same band. Then, as in Sec. III B of part II, one convenient way to account for that decomposition is to *subtract* from the transfer operator $\tilde{\mathbf{V}}(\hat{s}_m\hat{s}_{m-1})$, which adds $\hat{s}_m$ to the chain, the operator $\tilde{\mathbf{V}}(\underline{\hat{s}_m}s_{m-1}\cdots\underline{s_m}\hat{s}_{m-1})$ associated with adding the underlined spins: the argument of this latter operator is meant to indicate that it accounts for the two *interior*

*ends* of the two subchains that result when the chain constructed by $\tilde{\mathbf{V}}(\hat{s}_m\hat{s}_{m-1})$ is disconnected between bands $m$ and $m-1$. In this example, if $s_m s_{m-1}=0\,0$ and $\hat{s}_m\hat{s}_{m-1}=1\,1$, then the value of the operator $\tilde{\mathbf{V}}(\underline{\hat{s}_m}s_{m-1}\cdots\underline{s_m}\hat{s}_{m-1})$ is simply the product of the two Boltzmann factors $(00\to 10)$ and $(00\to 01)$, which, from (2.7)–(2.9), is $y\times y^{\theta}=y^{1+\theta}$. Therefore, to include all possible decompositions, one should replace the transfer operator $\tilde{\mathbf{V}}(\hat{s}\hat{s})=w_0\mathbf{B}'$ of (3.4) by

$$\mathbf{V}(\hat{s}\hat{s})\equiv\tilde{\mathbf{V}}(\hat{s}\hat{s})-\tilde{\mathbf{V}}(\hat{s}s\cdots s\hat{s})$$
$$\equiv w_0\mathbf{B}=w_0\begin{bmatrix}1-y^{1+\theta} & y^{\theta}-y^2\\ y-y^{2\theta} & 1-y^{1+\theta}\end{bmatrix}; \tag{3.9}$$

similarly, one must replace $\tilde{\mathbf{V}}(\hat{s}\,|\,\hat{s})=w_0\mathbf{C}'$ of (3.5) by

$$\mathbf{V}(\hat{s}\,|\,\hat{s})=\tilde{\mathbf{V}}(\hat{s}\,|\,\hat{s})-\tilde{\mathbf{V}}(\hat{s}\,|\,s\cdots s\,|\,\hat{s})$$
$$\equiv w_0\mathbf{C}=w_0\begin{bmatrix}1-y^{1-2\theta} & y^{1-\theta}-y^{-2\theta}\\ y^{-\theta}-y^{2-2\theta} & 1-y^{1-2\theta}\end{bmatrix}. \tag{3.10}$$

The four types of chains $1\nu'1$, $1\nu'2$, $2\nu'1$, and $2\nu'2$, with $\nu'\equiv 2^k$, including all their possible decompositions, can now be summed according to the signs given by Rule 1 of Sec. II to yield finally,[7] using (3.1),

$$\overline{W}_2(2k+1)=(\mathbf{c}_0^{\dagger}-\mathbf{b}_0^{\dagger})(\mathbf{CB})^k\mathbf{C}(\mathbf{b}_1-\mathbf{c}_1)w_0^{2k+2}$$
$$\times[1+O(kw^{q_0-2})]. \tag{3.11}$$

The error term here is dominated by the next-to-leading excited states, obtained from a leading excitation like (2.24) by flipping an additional spin which is an in-layer nearest neighbor to one of the flipped spins of the chain; as written, however, this error estimate is excessively large whenever $k$ exceeds order unity, as will be discussed in Sec. III B.

The three-wall interaction $\overline{W}_3(l,l)=(12^k12^k1)$ is given by an analogous sum of matrix products, the only difference being that now the core $\nu'$ of the four types of layer sequences entering Rule 1 is $\nu'\equiv 2^k12^k$, so that[7]

$$\overline{W}_3(2k+1,2k+1)=(\mathbf{c}_0^{\dagger}-\mathbf{b}_0^{\dagger})(\mathbf{CB})^k\mathbf{C}(\mathbf{CB})^k\mathbf{C}(\mathbf{b}_1-\mathbf{c}_1)w_0^{4k+3}[1+O(kw^{q_0-2})]. \tag{3.12}$$

The remark after (3.11) applies equally here.

To evaluate the indicated matrix products, note first that from the definitions (2.7)–(2.10), one can verify the identity

$$y^{\theta}=\exp\left[K_1\delta\cos\frac{2\pi}{3}\kappa\right]. \tag{3.13}$$

Consequently, on the $\langle 1\rangle$:$\langle 2\rangle$ pseudoboundary, $\delta=\delta_1^{(1)}(T)$, given by (2.13), one has (with $q_1=2$)

$$y^{\theta}=1+2(1-y)^2w_0+O(w^{2q_0-2}), \tag{3.14}$$

whence it is permissible to set $\theta=0$ as a first approximation in (3.11) and (3.12). (Further discussion of the validity of this simplification is presented below in Sec. III B.) The matrix to be iterated is then just[13]

$$\mathbf{CB}\equiv(1-y)^2\mathbf{D}=(1-y)^2\begin{bmatrix}2 & y\\ y & 2+2y+y^2\end{bmatrix}. \tag{3.15}$$

This matrix $\mathbf{D}$ is Hermitian with eigenvalues

$$\lambda_{\pm}(y)\equiv u(y)\pm y[v(y)]^{1/2},$$
$$u(y)=2+y+\tfrac{1}{2}y^2,\quad v(y)=2+y+\tfrac{1}{4}y^2, \tag{3.16}$$

and orthonormal eigenvectors

$$\mathbf{u}_{\pm}(y)=\frac{v^{-1/4}}{\sqrt{2}\,|\,1+\frac{1}{2}y\pm\sqrt{v}\,|^{1/2}}\begin{bmatrix}1\\ 1+\frac{1}{2}y\pm\sqrt{v}\end{bmatrix}. \tag{3.17}$$

Working in the basis of these eigenvectors, one concludes from (3.11) that[7]

$$\overline{W}_2(l)=w_0^{2k+2}(1-y)^{2k+3}[A_+\lambda_+^k+A_-\lambda_-^k]$$
$$\times[1+O(kw^{q_0-2})], \tag{3.18}$$

where $l=2k+1$ and the amplitudes are

$$A_{\pm}(y)=(1-y)^{-3}[(\mathbf{c}_0^{\dagger}-\mathbf{b}_0^{\dagger})\mathbf{u}_{\pm}][\mathbf{u}_{\pm}^{\dagger}\mathbf{C}(\mathbf{b}_1-\mathbf{c}_1)]\,|_{\theta=0}$$
$$=(1-\tfrac{1}{2}y)\mp(2+\tfrac{1}{2}y+\tfrac{1}{4}y^2)[v(y)]^{-1/2}, \tag{3.19}$$

where the dagger denotes the Hermitian conjugate matrix or vector. Similarly, (3.12) assumes the form

$$\overline{W}_3(l,l)=-w_0^{4k+3}(1-y)^{4k+4}[A_{++}\lambda_+^{2k}+A_{--}\lambda_-^{2k}+A_{+-}(\lambda_+\lambda_-)^k]\lambda_-^{2k}1+O(kw^{q_0-2})]. \tag{3.20}$$

By comparing this to (3.12) computed directly when $k=0$, one finds

$$A_{+-}=4y-A_{++}-A_{--}, \tag{3.21}$$

so that (3.20) can be alternatively written[7]

$$\overline{W}_3(l,l)=-w_0^{4k+3}(1-y)^{4k+4}[4y(\lambda_+\lambda_-)^k+(A_{++}\lambda_+^k-A_{--}\lambda_-^k)(\lambda_+^k-\lambda_-^k)][+O(kw^{q_0-2})], \tag{3.22}$$

where $l=2k+1$ and the remaining amplitudes are

$$A_{\pm\pm}(y)=-(1-y)^{-1}A_{\pm}(y)(\mathbf{u}_{\pm}^{\dagger}\mathbf{C}\mathbf{u}_{\pm})\,|_{\theta=0}$$
$$=-A_{\pm}(y)\left[1\pm\frac{y}{2[v(y)]^{1/2}}\right]. \tag{3.23}$$

With these explicit low-temperature forms for $\overline{W}_2$ and $\overline{W}_3$ in hand, one can now determine the phase diagram according to the program of I. To accomplish the initial refinement of the $\langle 1\rangle$:$\langle 2\rangle$ crossover regime, based on $\overline{W}_2(l)$ alone, first observe that over the entire range of values (0,1) accessible to the Boltzmann factor $y$ at nonzero temperatures, one has

$$0<\lambda_-(y)<\lambda_+(y) \tag{3.24}$$

and

$$A_-(y)>0,\quad A_+(y)<0,\quad A_-(y)>|A_+(y)|\ . \tag{3.25}$$

Consequently, $\overline{W}_2(l)$ has the form shown in Fig. 1, with a unique negative minimum at $l_{\max}=2k_{\max}+1$, where

$$k_{\max}(T)\simeq\ln\left[\frac{A_-\ln[w_0^2(1-y)^2\lambda_-]}{|A_+|\ln[w_0^2(1-y)^2\lambda_+]}\right]\Big/\ln(\lambda_+/\lambda_-)$$
$$=\sqrt{2}y^{-1}\ln(1+\sqrt{2})[1+O(k_BT/q_0J_0,y)]\ . \tag{3.26}$$

According to the classification of I, then, $\overline{W}_2(l)$ belongs to case B, and it is convex for $1\le l\le l_{\max}$. One therefore concludes that, among the simple periodic phases $\langle 12^k\rangle$, which display just a single interwall separation, only $\langle 12\rangle$, $\langle 12^2\rangle$, $\langle 12^3\rangle$, ..., $\langle 12^{k_{\max}}\rangle$ (with no gaps in the sequence) will be stable within the crossover regime near the $\langle 1\rangle$:$\langle 2\rangle$ pseudoboundary. Moreover, the maximum separation $k_{\max}(T)\sim y^{-1}\to\infty$ as $T\to 0$, so that the phase diagram is precisely that found by Yeomans and Fisher. (See Fig. 1 of Ref. 6 and Fig. 3 below.) Finally, note from (3.23) and (3.25) that one has

$$A_{++}(y)>0,\quad A_{--}(y)<0\ \text{ for all } 0<y<1\ , \tag{3.27}$$

whence, from (3.22), one obtains

$$\overline{W}_3(l,l)<0\ \text{ for all } l\ge 1\ . \tag{3.28}$$

According to Sec. V of part I, then, each $\langle 12^k\rangle$:$\langle 12^{k+1}\rangle$ boundary remains stable to *all* orders of the free-energy expansion (2.17). The phases shown in Fig. 2 are thus the *only* ones present at those temperatures low enough for (3.18) and (3.22) to be valid expressions for $\overline{W}_2$ and $\overline{W}_3$.

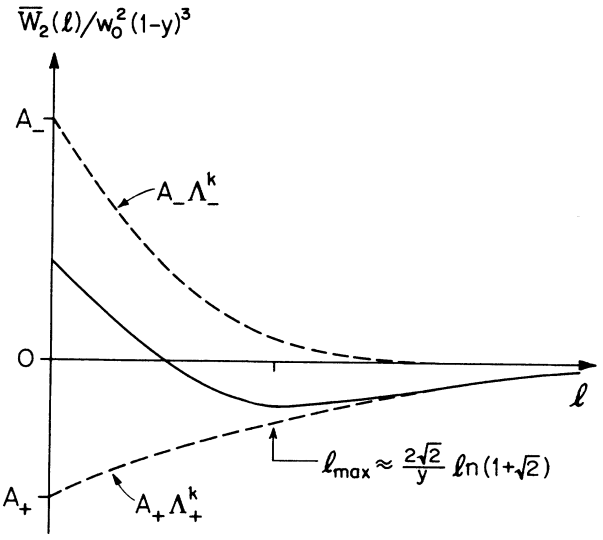


FIG. 1. Sketch of the pair interaction $\overline{W}_2(l)$ vs $l$ for the three-state chiral clock ($CC_3$) model, for axial coordination number $q_1=2$, as given by (3.18). Here we have put $\Lambda_{\pm}\equiv w_0^2(1-y)^2\lambda_{\pm}(y)$ while $l=2k+1$. The potential has a unique minimum and epitomizes case B of the general classification of I.

It was, of course, only to be expected that the results of this treatment should agree with the findings of Yeomans and Fisher. The advantage of the present approach, however, is that it reveals more clearly how the characteristics of the forces between domain walls are reflected in the appearance of the phase diagram. Also, it is readily generalized to alterations of the model, as will be explored in Sec. IV. First, however, we briefly discuss the nature of the corrections to these lowest-order results for $\overline{W}_2$ and $\overline{W}_3$.

### B. Higher-order corrections

Two approximations were made in our calculation of domain wall interactions in Sec. III A: (i) setting $y^{\theta}\equiv 1$ in the matrix products (3.11) and (3.12); (ii) neglecting higher-order excited states containing more flipped spins than are present in the axial chains like (2.24). Regarding approximation (i), it was noted in (3.14) that the corrections are of order $w_0$, which is always assumed to be much smaller than unity. The eigenvalues $\lambda_{\pm}$ of the matrix $\mathbf{D}\propto\mathbf{CB}$, however, are separated by an amount $2y[v(y)]^{1/2}=O(y)$, according to (3.16). Now when correction terms of order $w_0$ are added to each of the matrix elements of $\mathbf{D}$ in (3.15), the gap between eigenvalues will be altered by a term of order $(yw_0)^{1/2}$: for such a correction to be negligible, one must have

$$y\gg w_0\ \text{ or } q_0J_0>J_1\ . \tag{3.29}$$

In fact, as established in Sec. IV D, this type of correction would drive $v(y)$ *negative* in the anisotropic regime where (3.29) fails, thus making $\lambda_{\pm}$ *complex* eigenvalues. [See Fig. 2(b), below, where $\Delta\equiv y$ for $q_1=2$.] The two-wall interaction $\overline{W}_2(l)$ would then be an exponentially damped sinusoidal function of $l$. Such a form still exhibits a negative absolute minimum and so still belongs to the classification of case B. Consequently, the phase diagram of the $CC_3$ model would continue to exhibit a harmless staircase with only finitely many $\langle 12^k\rangle$ phases at any fixed temperature, although the quantitative details of the phase diagram would of course be altered.

These corrections due to the nonzero value of $\theta$ are, however, overshadowed by the corrections arising from higher-order excited states. The contributions of these states can be incorporated in the transfer-matrix notation used here, at the expense of introducing larger matrices, as discussed in Sec. VI of part I. For example,

suppose it is desired to account for the leading correction

$$|\hat{s}\,|\hat{s}\hat{s}\,|\hat{s}\hat{s}\,\Big|\begin{matrix}\hat{s}\\ \hat{s}\hat{s}\end{matrix}|\hat{s}\hat{s}\,|\,\cdots\,|\hat{s}\hat{s}\,|\hat{s}\,|\,, \tag{3.30}$$

where an extra in-layer nearest neighbor to one of the spins in the chain is flipped. Note that since the leading excited state has *every* spin in the chain flipped, the leading correction must be constructed by flipping an extra *in-layer* NN, in any of the $2k+2$ layers of the chain. This is a significant difference from the ANNNI model, where (because of the second-neighbor axial couplings) the leading excited state had only every *second* spin in the chain flipped, and the leading correction came from flipping an extra *in-chain* spin: see Sec. III C of part II. To accommodate states like (3.30), for either of the two values to which a spin $s_m$ of the chain may be flipped, one must allow for three possibilities: either $s_m$ is the only spin flipped in layer $m$, or one of its $q_0$ in-layer NN spins, $s'_m$, may also be flipped to one of *two* other values. This enlarged number of possible states requires that each of the *elements* $b_{ij}$ of the matrix **B** (and similarly for the matrix **C**) be replaced by a $3\times 3$ *matrix*, $\mathbf{B}_{ij}$, whose $(k,l)$th entry is the relative Boltzmann factor for the change

$$\begin{Bmatrix} s'_m & s'_{m-1}\\ s_m & s_{m-1}\end{Bmatrix}\rightarrow\begin{Bmatrix}(s'_m+k)(\mathrm{mod}3) & (s'_{m-1}+l)(\mathrm{mod}3)\\ (s_m+i)(\mathrm{mod}3) & (s_{m-1}+j)(\mathrm{mod}3)\end{Bmatrix}\quad\text{for } k,l=0,\ 1,\ \text{or } 2\ . \tag{3.31}$$

Here it has been assumed that $s'_m$ and $s'_{m-1}$ will not be axial NN, so that there is no interaction between them. To include the possibility of such interactions, one would have to make each $\mathbf{B}_{ij}$ $5\times 5$; indeed, in the limit where all possible excited states of the layer $m$ are to be included, each $\mathbf{B}_{ij}$ would become infinite-dimensional. Note, however, that the corner element of each $\mathbf{B}_{ij}$ is simply $(\mathbf{B}_{ij})_{00}=b_{ij}$.

Now the matrix $\mathbf{D}\propto\mathbf{CB}$, thus enlarged, will, in the appropriate basis, exhibit the form

$$\mathbf{D}=\begin{bmatrix}\lambda_+ & & & & & \\ & 0 & & 0 & & \\ & & 0 & & & \\ & & & \lambda_- & & \\ & 0 & & & 0 & \\ & & & & & 0\end{bmatrix}+w^{q_0-2}\mathbf{D}'\ , \tag{3.32}$$

where $\lambda_\pm(y)$ are the eigenvalues (3.16) of the original $2\times 2$ matrix, and $\mathbf{D}'$ is a $6\times 6$ matrix with elements of order unity, embodying the effects of the higher-order excited states. It is clear from this form that **D** will possess two largest eigenvalues, $\lambda_{1,2}\equiv\lambda'_\pm$, close to the original eigenvalues $\lambda_\pm$, as well as several smaller eigenvalues $\lambda_i=O(\lambda_\pm w^{q_0-2})$ for $i=3,4,5,\ldots$. Hence, the two-wall interaction will still exhibit the general form

$$\overline{W}_2(l)=w_0^{2k+2}\left[A'_+\lambda'^k_+ + A'_-\lambda'^k_- + \sum_{i\geq 3}A_i\lambda_i^k\right]\ , \tag{3.33}$$

with corresponding forms for $\overline{W}_n$, $n\geq 3$. Because of the factor $w^{q_0-2}$ multiplying $\mathbf{D}'$ in (3.32), the principal eigenvalues $\lambda'_\pm$ and amplitudes $A'_\pm$ in $\overline{W}_2(l)$ may be found using perturbation theory, without resorting to a complete diagonalization of **D**. Although this analysis is not carried out here, comparison of (3.33) with (3.18) reveals that the correction factor $[1+O(kw^{q_0-2})]$ given in (3.18) must simply be the leading term in an expansion of $(\lambda'_+/\lambda_+)^k$ or $(\lambda'_-/\lambda_-)^k$, i.e.,

$$\lambda'_\pm=\lambda_\pm+O(w^{q_0-2})\ . \tag{3.34}$$

Now, as noted above, such a correction to $\lambda_\pm$ will become significant, perhaps even transforming $\lambda_\pm$ into complex conjugate eigenvalues, when it is of the order of the gap $2y[v(y)]^{1/2}=O(y)$ between $\lambda_\pm$. Conversely, one may *neglect* these corrections from higher-order excited states *provided*

$$y\gg w^{q_0-2}\quad\text{for } (q_0-2)J_0>J_1\ . \tag{3.35}$$

In that case, (3.18) overestimates the error when $k$ exceeds order unity, and the proper form for all $k$ is as given by (3.33) and (3.34). Notice that the condition (3.29), required to ensure the validity of the approximation $\theta=0$, is automatically satisfied whenever (3.35) holds: the inequality (3.35) thus gives the fundamental limitation on the results presented here. Observe that the model with isotropic couplings on a simple cubic lattice ($J_0=J_1$, $q_0=4$), which is most commonly adopted for numerical studies, is admitted by (3.35).

## IV. ARBITRARY COORDINATION NUMBERS AND THE MEAN-FIELD LIMIT

### A. Pair interactions and quasitricritical point

The results presented so far apply for general in-layer coordination number $q_0$, but the axial coordination number is restricted to the simplest case $q_1=2$. One would like to obtain expressions valid for general $q_1$, in part to permit examination of the limit $q_i\rightarrow\infty$ with $q_iJ_i$ constant ($i=0,1$), in which mean-field theory becomes exact. This requires alteration of the transfer matrices **B** and **C** which describe the addition of one more flipped spin $\hat{s}_m$ to the left end of the axial chain of flipped spins. Observe that $\hat{s}_m$ can occupy $\frac{1}{2}q_1$ positions relative to $\hat{s}_{m-1}$. Upon adding $\hat{s}_m$ to the chain, one must account, as usual, for the $q_0$ in-layer broken bonds surrounding it, but also for: (i) the single bond between $\hat{s}_m$ and $\hat{s}_{m-1}$; (ii) the $\frac{1}{2}q_1-1$ remaining axial bonds between $\hat{s}_m$ and *un*flipped spins in layer $m-1$; (iii) the $\frac{1}{2}q_1-1$ remaining axial bonds between $\hat{s}_{m-1}$ and unflipped spins in layer $m$. If the chain is to be disconnected between $\hat{s}_m$ and

$\hat{s}_{m-1}$, then the bond of type (i) no longer exists, but there are now $\frac{1}{2}q_1$ bonds of types (ii) and (iii). As an example, then, consider the entry $b_{11}$ of the matrix **B**, which gives the Boltzmann factor for the case where $s_m$ and $s_{m-1}$ are in the same band (say, $s_m = s_{m-1} = 0$) and are both flipped to $\hat{s}_m = \hat{s}_{m-1} = 1$. For arbitrary $q_1$, one has, using the Boltzmann factors (2.7)–(2.9),

$$b_{11} = \tfrac{1}{2}q_1(1 \times y^{q_1/2-1} \times y^{\theta(q_1/2-1)} - y^{q_1/2} \times y^{\theta q_1/2}) = \tfrac{1}{2}q_1 \tilde{y}^{1+\theta}(1-y^{1+\theta}) , \tag{4.1}$$

where the abbreviation

$$\tilde{y} \equiv y^{q_1/2-1} \tag{4.2}$$

has been introduced and will be used henceforth. Notice that for $q_1 = 2$ one simply has $\tilde{y} \equiv 1$.

In the same fashion, one can construct all the elements of **B** [compare (3.9)], of the matrix **C** which describes the case where $\hat{s}_m$ and $\hat{s}_{m-1}$ are separated by a band edge [see (3.10)], and of the row and column vectors $\mathbf{b}_i$, $\mathbf{c}_i$ $(i = 0, 1)$ which account for the broken bonds at the ends of the chain [see (3.6) and (3.7)]. The results are

$$\mathbf{B} = \tfrac{1}{2}q_1 \begin{bmatrix} \tilde{y}^{1+\theta}(1-y^{1+\theta}) & \tilde{y}^{2}(y^{\theta}-y^{2}) \\ \tilde{y}^{2\theta}(y-y^{2\theta}) & \tilde{y}^{1+\theta}(1-y^{1+\theta}) \end{bmatrix} , \tag{4.3}$$

$$\mathbf{C} = \tfrac{1}{2}q_1 \begin{bmatrix} \tilde{y}^{1-2\theta}(1-y^{1-2\theta}) & \tilde{y}^{-2\theta}(y^{1-\theta}-y^{-2\theta}) \\ \tilde{y}^{2(1-\theta)}(y^{-\theta}-y^{2(1-\theta)}) & \tilde{y}^{1-2\theta}(1-y^{1-2\theta}) \end{bmatrix} , \tag{4.4}$$

$$\mathbf{b}_0^{\dagger} = [(y\tilde{y})^{\theta},\ y\tilde{y}],\quad \mathbf{c}_0^{\dagger} = [(y\tilde{y})^{1-\theta},\ (y\tilde{y})^{-\theta}] , \tag{4.5}$$

$$\mathbf{b}_1 = \begin{bmatrix} y\tilde{y} \\ (y\tilde{y})^{\theta} \end{bmatrix},\quad \mathbf{c}_1 = \begin{bmatrix} (y\tilde{y})^{-\theta} \\ (y\tilde{y})^{1-\theta} \end{bmatrix} . \tag{4.6}$$

These then are the matrices and vectors to be substituted into the expressions (3.11) and (3.12) determining $\overline{W}_2(l)$ and $\overline{W}_3(l,l)$. As before, one would like to simplify the algebra by setting the exponent $\theta = 0$. On the $\langle 1 \rangle : \langle 2 \rangle$ pseudoboundary $\delta = \delta_1^{(1)}(T)$, given by (2.13), one deduces from the definitions (3.13) and (4.2) that

$$(y\tilde{y})^{\theta} \equiv y^{q_1\theta/2} = 1 + 2(1-y\tilde{y})^2 w_0 + O(w^{2q_0-2}) , \tag{4.7}$$

and hence also

$$\tilde{y}^{\theta} \equiv (y\tilde{y})^{\theta(1-2/q_1)} = 1 + 2(1-2/q_1)(1-y\tilde{y})^2 w_0 + O(w^{2q_0-2}) . \tag{4.8}$$

It is therefore permissible to set $\theta = 0$ in all the terms of (4.3)–(4.6), up to corrections of order $w_0$ whose effects will be investigated in Sec. IV D. This statement holds even in the limit $q_1 \to \infty$, provided $q_1 J_1$ is kept constant, for then, from the definition (2.12),

$$y\tilde{y} \equiv y^{q_1/2} \equiv w^{q_1 J_1/[2J_0(1-\theta+\theta^2)^{1/2}]} \tag{4.9}$$

remains fixed while $y \to 1$.

On setting $\theta = 0$ the matrix to be iterated in (3.11) and (3.12) is thus just

$$\mathbf{CB} \equiv \tfrac{1}{4}q_1^2(1-y)^2\mathbf{D} = \tfrac{1}{4}q_1^2(1-y)^2 \begin{bmatrix} 1+\tilde{y}^2 & \tilde{y}\Delta \\ \tilde{y}\Delta & 1+\tilde{y}^2+\Delta(2+\Delta) \end{bmatrix} , \tag{4.10}$$

where

$$\Delta(y; q_1) \equiv \tilde{y}^2(1+y) - 1 . \tag{4.11}$$

This is to be compared with (3.15), which is valid when $q_1 = 2$, or $\tilde{y} \equiv 1$ and $\Delta = y$. Now as $q_1$ increases from 2, $\tilde{y}$ decreases from 1 exponentially fast. (Note that $\tilde{y} = y$ at $q_1 = 4$.) Hence $\Delta$ quickly decreases from $y$, through $\Delta = 0$, toward $\Delta = -1$. Observe that there is a special degeneracy *at* $\Delta = 0$, where the matrix **D** becomes proportional to the identity matrix. This special point $\Delta = 0$ marks a *quasitricritical point* of crossover between two regimes of qualitatively different behavior in the $CC_3$ model, as discussed in Sec. VII of part I [compare (4.10) with Eq. (7.2) of I]. We now examine the details of this quasitricriticality in the $CC_3$ model.

The matrix **D** is again Hermitian, with eigenvalues

$$\lambda_{\pm} \equiv u(y) \pm \Delta[v(y)]^{1/2}$$
$$u(y) = 1 + \tilde{y}^2 + \Delta(1+\tfrac{1}{2}\Delta),\quad v(y) = (1+\tfrac{1}{2}\Delta)^2 + \tilde{y}^2 , \tag{4.12}$$

and orthonormal eigenvectors

$$\mathbf{u}_{\pm}(y) = \frac{v^{-1/4}}{\sqrt{2}\,|\,1+\tfrac{1}{2}\Delta \pm \sqrt{v}\,|^{1/2}} \begin{bmatrix} \tilde{y} \\ 1+\tfrac{1}{2}\Delta \pm \sqrt{v} \end{bmatrix} . \tag{4.13}$$

Working in this basis of eigenvectors, one obtains from (3.11) a result for $\overline{W}_2(l)$ analogous to (3.18) and (3.19), namely,

$$\overline{W}_2(l) = w_0^{2k+2}(1-y\tilde{y})^2[\tfrac{1}{2}q_1(1-y)]^{2k+1} \times (A_+\lambda_+^k + A_-\lambda_-^k)[1+O(kw^{q_0-2})] \tag{4.14}$$

with $l = 2k+1$ and amplitudes

$$A_{\pm}(y) = (\tilde{y} - \tfrac{1}{2}\Delta) \mp [\tilde{y}(\tilde{y} - \tfrac{1}{2}\Delta) + (1+\tfrac{1}{2}\Delta)^2][v(y)]^{-1/2} . \tag{4.15}$$

In these expressions, one can easily check that for all $y$ in the physical domain (0,1), and regardless of the sign of $\Delta$, one has

$$A_-(y) > 0,\quad A_+(y) < 0,\quad A_-(y) > |\,A_+(y)\,| . \tag{4.16}$$

However, as shown in Fig. 2(a), the eigenvalues $\lambda_{\pm}$ *cross* at $\Delta = 0$, with

$$0 < \lambda_-(y) < \lambda_+(y) \quad \text{for } \Delta > 0 ,$$
$$0 < \lambda_+(y) < \lambda_-(y) \quad \text{for } \Delta < 0 . \tag{4.17}$$

Consider first $\Delta > 0$. Here $\overline{W}_2(l)$ exhibits the same type of case B behavior found earlier for $q_1 = 2$ (recall Fig. 1), where now the minimum of $\overline{W}_2(l)$ occurs at $l_{\max} = 2k_{\max} + 1$ with

$$k_{\max}(T) \simeq (1+\tilde{y}^2)^{1/2}\Delta^{-1}\ln[\tilde{y} + (1+\tilde{y}^2)^{1/2}] \times [1 + O(k_B T/q_0 J_0, y)] . \tag{4.18}$$

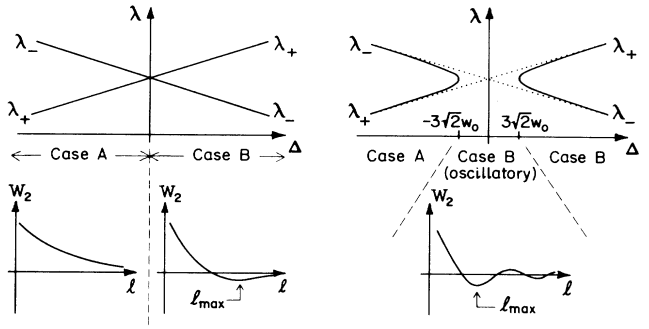


FIG. 2. Variation of the $CC_3$ transfer-matrix eigenvalues $\lambda_\pm$ with the parameter $\Delta$ defined in (4.11). To leading order (i.e., setting the exponent $\theta \equiv 0$ and neglecting out-of-chain spin flips), the eigenvalues cross at $\Delta = 0$, as shown in (a): for $\Delta > 0$, the resulting two-wall interaction $W_2(l)$ exhibits case B behavior (having a unique negative minimum); for $\Delta < 0$, $W_2(l)$ belongs to case A (being everywhere positive). Accounting just for a small, nonzero value of $\theta$ would split the degeneracy at $\Delta = 0$ and drive the eigenvalues complex in the narrow region $|\Delta| < 3\sqrt{2}w_0$, as shown in (b): within this crossover region, $W_2(l)$ would therefore be oscillatory (hence again of case B). Such a correction may, however, be overshadowed by the contribution from out-of-chain spin flips in the slightly larger region $|\Delta| \lesssim w^{q_0-2}$.

For $\Delta < 0$, on the other hand, one has $\overline{W}_2(l) > 0$ for all $k \geq 0$ [see Fig. 2(a)], placing it within case A of I. Now the most physically relevant situation is of course to consider a *fixed* axial coordination number $q_1 > 2$; then

$$y,\ \tilde{y} \to 0 \quad \text{and} \quad \Delta \to -1 \quad \text{as} \quad T \to 0\ , \qquad y,\ \tilde{y} \to 1 \quad \text{and} \quad \Delta \to 1 \quad \text{as} \quad T \to \infty\ , \tag{4.19}$$

whence the phase diagram of the model in the $(\kappa, T)$ plane must exhibit a *crossover* between these case B and case A regimes, at the particular temperature $T \equiv T_1(q_1)$ where $\Delta = 0$. This is illustrated in Fig. 3. At temperatures $T < T_1$, where $\Delta < 0$, the model exhibits a "devil's last step" with *all* simple periodic phases $\langle 12^k \rangle$, $k \geq 1$, appearing between $\langle 1 \rangle$ and $\langle 2 \rangle$. But for $T > T_1$, where $\Delta > 0$, only those phases with $k \leq k_{\max}$ are stable: the cutoff $k_{\max}$, given by (4.18), diverges as $\Delta \to 0+$, and one recovers a picture like that found by Yeomans and Fisher[6,7] for the case $q_1 = 2$ (compare Fig. 1 of Ref. 6).

The point at $\Delta = 0$ on the $\langle 2 \rangle$ phase boundary thus marks a quasitricritical point, separating the *quasicontinuous* $\langle 2 \rangle$ boundary at lower temperatures from the *first-order* $\langle 2 \rangle$ boundary at higher temperatures. Higher-order correction terms to the elements of the matrix **D** in (4.10) may shift the location of this quasitricritical point slightly away from $\Delta = 0$, and may also, possibly, introduce a new *pair* of such quasitricritical points nearby, as discussed in Sec. VII of part I and in Sec. IV D below. The "crossover region" in which these higher-order effects may occur is of width $O(w^{q_0-2})$ in $\Delta$: only those $\langle 12^k \rangle$ phases with large $k$ in Fig. 3 (i.e., near $\langle 2 \rangle$) can be affected.

It should be noted, however, that the crossover temperature $T_1$, determined by the locus $\Delta = 0$, or

$$\tilde{y}^2 \equiv y^{q_1-2} = (1+y)^{-1}\ , \tag{4.20}$$

is in practice a relatively high temperature. Physically, the axial coordination number $q_1$ must be an even integer, so $q_1 = 4$ is the smallest value which exceeds $q_1 = 2$. As $q_1$ increases from 4 to $\infty$, the value of $\tilde{y}$ determined by (4.20) decreases from 0.755 to $1/\sqrt{2} \simeq 0.707$, corresponding to a temperature range for $T_1$ of

$$2.667 \gtrsim k_B T_1 / [(q_1 - 2) J_1] \gtrsim 2.164\ . \tag{4.21}$$

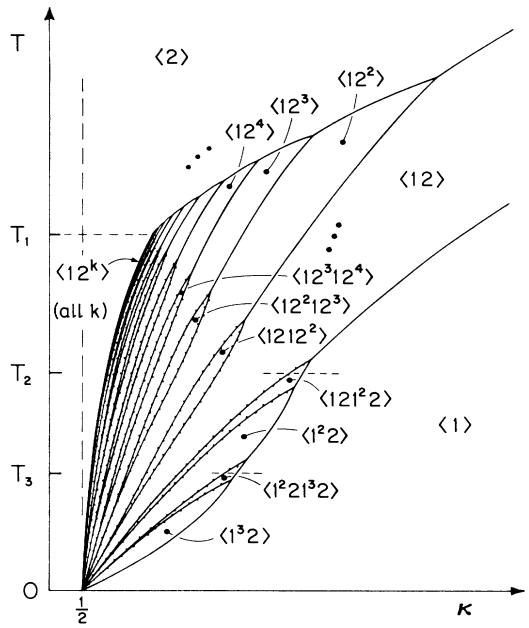


FIG. 3. Schematic phase diagram of the $CC_3$ model for arbitrary axial coordination number $q_1 > 2$, in the plane of chiral field $\kappa$ vs temperature $T$, as deduced under the low-temperature condition $w_0 = \exp(-3q_0 J_0 / 2k_B T) \ll 1$. The entire phase diagram is symmetric under reflection in the axis $\kappa = \frac{1}{2}$; only the region $\kappa \geq \frac{1}{2}$ is shown. Several distinct regimes are encountered, reflecting the presence of a quasitricritical point on the $\langle 2 \rangle$ phase boundary at $T = T_1$. First, for $T > T_1$, only simple periodic phases $\langle 12^k \rangle$ with $1 \leq k \leq k_{\max}$ are present between $\langle 1 \rangle$ and $\langle 2 \rangle$, where $k_{\max} \to \infty$ as $T \to T_1$; each $\langle 12^k \rangle$:$\langle 12^{k+1} \rangle$ boundary is stable and *no* other phases appear. When $q_1$ approaches 2 one has $T_1 \equiv 0$ and the phase diagram reduces to that originally found by Yeomans and Fisher (Refs. 6 and 7) for the simple cubic lattice (with $q_1 = 2$). Second, for fixed $T < T_1$, *all* phases $\langle 12^k \rangle$, $k \geq 1$, are present between $\langle 1 \rangle$ and $\langle 2 \rangle$. For $T < T_2$, each $\langle 12^k \rangle$:$\langle 12^{k+1} \rangle$ phase boundary ($k \geq 0$) is unstable to the mixed phase $\langle 12^k 12^{k+1} \rangle$ and, possibly, to other phases that may arise on the associated phase boundaries (which are therefore decorated with dots): in particular, the existence of $\langle 1^3 2 \rangle$ for $T < T_3$ and also of $\langle 121^2 2 \rangle$ and $\langle 1^2 21^3 2 \rangle$, is established. The mixed phases $\langle 12^k 12^{k+1} \rangle$ successively close off, however, as $T$ increases from $T_2$ to $T_1$. Phase widths, which decrease exponentially fast as $k$ increases, have been exaggerated for clarity. Finally, the phase diagram remains qualitatively valid as $q_1$ is increased to $\infty$, which generates the mean-field limit.

On the other hand, recall that one always requires $w_0 \ll 1$, or $k_B T \ll q_0 J_0$, to ensure the validity of the low-temperature forms employed here for the $\overline{W}_n$. Consequently, the predicted phase diagram for temperatures $T \geq T_1$ is reliable only for highly *anisotropic* systems satisfying

$$q_0 J_0 \gg k_B T \sim q_1 J_1 \ . \tag{4.22}$$

For the more commonly considered isotropic systems, the case A regime with devil's last step behavior will dominate the low-temperature phase diagram.

### B. Triplet interactions and mixed phases

For further refinements of these phase diagrams, one needs the three-wall interaction $\overline{W}_3(l,l)$. The expressions analogous to (3.22) and (3.23) which one obtains are

$$\overline{W}_3(l,l) = -w_0^{4k+3}(1-y\bar{y})^2[\tfrac{1}{2}q_1(1-y)]^{4k+2} \times\{(A_{++}\lambda_+^k - A_{--}\lambda_-^k)(\lambda_+^k-\lambda_-^k) - 2\bar{y}(1+\bar{y})[1-\bar{y}(1+y)](\lambda_+\lambda_-)^k\}[1+O(kw^{q_0-2})] \ , \tag{4.23}$$

with $l = 2k+1$ while the amplitudes are

$$A_{\pm\pm}(y) = -\bar{y}A_{\pm}(y)\left[1 \pm \frac{\Delta}{2[v(y)]^{1/2}}\right] \ . \tag{4.24}$$

Insofar as the factor in large parentheses here is always positive, regardless of the sign of $\Delta$, one obtains from (4.16),

$$A_{++}(y) > 0, \quad A_{--}(y) < 0 \ . \tag{4.25}$$

For all $\Delta > 0$ one has $\lambda_- < \lambda_+$ and the factor $[1-\bar{y}(1+y)]$ in (4.23) is negative. Consequently, one concludes

$$\overline{W}_3(l,l) < 0 \quad \text{for all } l \geq 1 \quad (\Delta > 0) \ . \tag{4.26}$$

The simple periodic phases $\langle 12^k \rangle$ are therefore the *only* stable phases between $\langle 1 \rangle$ and $\langle 2 \rangle$ when $\Delta$ is positive ($T > T_1$), again in agreement with the $q_1 = 2$ phase diagram of Yeomans and Fisher.[6,7]

For $\Delta < 0$ or $T < T_1$, however, the situation is somewhat more complex. One now has $\lambda_- > \lambda_+$, whence the large-$l$ behavior of $\overline{W}_3(l,l)$ is dominated by the term $A_{--}\lambda_-^{2k}$ within the braces in (4.23), so that $\overline{W}_3(l,l) > 0$ for all sufficiently large $l$. But if $\bar{y}(1+y) > 1$, then $\overline{W}_3(1,1) < 0$, so that there must exist a border value $l = l^\dagger > 1$ at which $\overline{W}_3(l,l)$ changes sign. Thus for $\Delta < 0$ we conclude

$$\begin{aligned} \overline{W}_3(l,l) &> 0 \quad \text{for all } l \geq 1 \quad \text{if (i)} \quad \bar{y}(1+y) < 1 \ , \\ &< 0 \quad \text{for } 1 \leq l < l^\dagger(y) \ , \\ &> 0 \quad \text{for all } l > l^\dagger(y) \quad \text{if (ii)} \quad \bar{y}(1+y) > 1 \ . \end{aligned} \tag{4.27}$$

The border value $l = l^\dagger(y)$ attains its minimum, $l^\dagger = 1$, at $\bar{y}(1+y) = 1$, which defines a temperature, $T \equiv T_2(q_1)$, below which $\overline{W}_3(l,l) > 0$ for all $l \geq 1$, and hence, according to Sec. V of part I, *every* $\langle 12^k \rangle : \langle 12^{k+1} \rangle$ pseudoboundary for $k = 0, 1, 2, \ldots$ is *unstable* to the appearance of the "mixed" phase $\langle 12^k 12^{k+1} \rangle$: see Fig. 3 and note that the presence of the $\langle 112 \rangle$ phase is implied by the argument. As $T$ increases from $T_2$, the border value $l^\dagger$ increases to $l^\dagger = \infty$ at $\bar{y}^2(1+y) = 1$ or $\Delta = 0$ ($T = T_1$); consequently, the mixed phases $\langle 12^k 12^{k+1} \rangle$ for successive values of $k \to \infty$ become cut off, as shown in Fig. 3.

To continue the refinement of the phase diagram as outlined in Sec. V of part I, one must check in turn the stability of the new $\langle 12^k \rangle : \langle 12^k 12^{k+1} \rangle$ and $\langle 12^k 12^{k+1} \rangle : \langle 12^{k+1} \rangle$ boundaries against the possible appearance of the phases $\langle 12^k 12^k 12^{k+1} \rangle$ and $\langle 12^k 12^{k+1} 12^{k+1} \rangle$, respectively, and then repeat the process, until either a complete devil's staircase is constructed or some negative $\overline{W}_n$ is encountered. This further checking, which requires knowledge of $\overline{W}_n$ for $n \geq 4$, has not been attempted here, except for the $\langle 1 \rangle : \langle 112 \rangle$ and $\langle 112 \rangle : \langle 12 \rangle$ pseudoboundaries (i.e., $k = 0$). Further analysis of those pseudoboundaries is easily made by adopting the point of view opposite to the one we have so far maintained, namely, by regarding the system as composed of 2-*band* walls separating $\langle 1 \rangle$-*phase* domains. By pursuing this line of inquiry, in Sec. IV C below, we demonstrate, as shown in Fig. 3, that the only additional phase of the form $\langle 1^k 2 \rangle$ which appears besides $\langle 12 \rangle$ and $\langle 1^2 2 \rangle$ is $\langle 1^3 2 \rangle$ (between $\langle 1 \rangle$ and $\langle 1^2 2 \rangle$). Furthermore, the $\langle 12 \rangle : \langle 1^2 2 \rangle$ and $\langle 1^2 2 \rangle : \langle 1^3 2 \rangle$ pseudoboundaries open to admit the intermediate phases $\langle 121^2 2 \rangle$ and $\langle 1^2 21^3 2 \rangle$ and, possibly, others (on the pseudoboundaries decorated with dots in Fig. 3).

Notice, finally, that the locus $\bar{y}(1+y) = 1$ mentioned in (4.27) is, like the locus $\Delta = 0$ or $\bar{y}^2(1+y) = 1$, effectively a high-temperature locus: to attain it within the restrictions of the present low-temperature analysis requires working in the anisotropic regime (4.22). Specifically, as $q_1$ increases from 4 to $\infty$, the value of $\bar{y}$ for which $\bar{y}(1+y) = 1$ decreases from $\frac{1}{2}(\sqrt{5}-1) \simeq 0.618$ to $\frac{1}{2}$, corresponding to a variation in $k_B T/[(q_1-2)J_1]$ only between 1.559 and 1.082—compare (4.21). Therefore, in isotropic systems, the correct low-temperature behavior is given by the lower part of the phase diagram in Fig. 3, where *all* $\langle 12^k \rangle$ phases, $k \geq 0$, are encountered up to a devil's last step, and *each* $\langle 12^k \rangle : \langle 12^{k+1} \rangle$ pseudoboundary is unstable to $\langle 12^k 12^{k+1} \rangle$ and, possibly, further phases.

### C. Further resolution of the $\langle 1 \rangle$ phase boundary

We now carry the resolution of the phase diagram somewhat further than was established above, by reversing the (arbitrary) point of view hitherto adopted, and

regarding the 2 *bands* as walls separating $\langle 1\rangle$-*phase* domains. Calculation of successive $n$-wall interactions (denoted $\tilde{W}_n$ to distinguish them from the previous $\overline{W}_n$ of this section) will then readily establish which phases of the form $\langle 1^k 2\rangle, \langle 1^k 21^{k+1}2\rangle$, etc., are stable. Hence, already at the level of the two-wall interaction $\tilde{W}_2$, these results will show whether or not all phases of the form $\langle 1^k 2\rangle$ appear between $\langle 1\rangle$ and $\langle 1^2 2\rangle$ in Fig. 3; at the level of $\tilde{W}_3$, the $\langle 12\rangle$:$\langle 1^2 2\rangle$ pseudoboundary can be tested for the presence of $\langle 121^2 2\rangle$.

The reasoning which led to the general transfer matrix expression (3.11) for $\overline{W}_2(l)$ can be carried over almost completely for the new interaction $\tilde{W}_2(l)$ between two 2-band walls separated by $k$ 1 bands: notice that the separation between walls is now $l=k+2$ lattice units. The main difference is that the transfer matrix to be iterated is no longer $w_0^2\mathbf{CB}$ (describing the addition of another 2 band to the chain), but simply $w_0\mathbf{C}$, which adds 1 bands to the chain [see (3.10)]. Thus one can immediately write down

$$\tilde{W}_2(k+2)=(\mathbf{c}_0^\dagger-\mathbf{b}_0^\dagger)\mathbf{C}^{k+1}(\mathbf{b}_1-\mathbf{c}_1)w_0^{k+2}[1+O(w_0)]\ . \tag{4.28}$$

For arbitrary $q_1$ and in leading order, where one can set $\theta=0$, the matrix $\mathbf{C}$ given by (4.4) has two *complex* eigenvalues

$$\tilde{\lambda}_\pm(y)\equiv\tfrac{1}{2}q_1(1-y)\bar{y}[1\pm i(1+y)^{1/2}]\ . \tag{4.29}$$

Hence one easily obtains

$$\tilde{W}_2(l)\approx\frac{w_0}{\bar{y}(1+y)^{1/2}}(1-y\bar{y})^2[1+\bar{y}^2(1+y)][\tfrac{1}{2}q_1(1-y)\bar{y}(2+y)^{1/2}w_0]^{k+1}\cos[(k+1)\Omega+\phi]\ , \tag{4.30}$$

with $l=k+2$, while

$$\tan\Omega=(1+y)^{1/2}\ \text{ and }\ \tan\phi=\Delta/2\bar{y}(1+y)^{1/2}\ . \tag{4.31}$$

Now $\tilde{W}_2(l)$ oscillates within an exponentially decaying envelope, like the example illustrated in Fig. 2(b): notice, however, that since $\Omega$ varies only from $\frac{1}{4}\pi$ at $y=0$ to $0.304\pi$ at $y=1$, the first (and absolute) minimum of $\tilde{W}_2(l)$ always occurs at $l_{\max}=k_{\max}+2$ with $k_{\max}$ not far from unity! More concretely, consider the results

$$\begin{aligned}\tilde{W}_2(2)&\simeq\tfrac{1}{2}q_1w_0^2(1-y)(1-y\bar{y})^2[1+2\bar{y}-\bar{y}^2(1+y)]\ ,\\ \tilde{W}_2(3)&\simeq\tfrac{1}{2}q_1^2w_0^3\bar{y}(1-y)^2(1-y\bar{y})^2(1+\bar{y})[1-\bar{y}(1+y)]\ .\end{aligned} \tag{4.32}$$

It is easy to check

$$\tilde{W}_2(2)>0\ \text{ for all } y,\ \bar{y}\in(0,1)\ . \tag{4.33}$$

Consequently, $k_{\max}$ must exceed zero, so that the simple periodic phase $\langle 1^k 2\rangle$ with $k=1$, namely, $\langle 12\rangle$, must always appear between $\langle 1\rangle$ and $\langle 2\rangle$, in agreement with what has already been deduced and displayed in Fig. 3. Furthermore, (4.32) implies

$$\begin{aligned}\tilde{W}_2(3)&>0\ \text{ if (i) }\ \bar{y}(1+y)<1\\ &<0\ \text{ if (ii) }\ \bar{y}(1+y)>1\ ,\end{aligned} \tag{4.34}$$

so that the phase with $k=2$, $\langle 112\rangle$, must also appear in case (i), $\bar{y}(1+y)<1$, again in agreement with the result embodied in Fig. 3. For (ii), $\bar{y}(1+y)>1$, however, the fact that $\tilde{W}_2(3)<0$ implies that the absolute negative minimum of $\tilde{W}_2(l)$ must be located at $l_{\max}=k_{\max}+2=3$, insofar as $\tilde{W}_2(l)$ carries the rapidly decaying prefactor $w_0^l$. Thus, in case (ii), one concludes that $\langle 12\rangle$ is the *only* phase of the form $\langle 1^k 2\rangle$ appearing between $\langle 1\rangle$ and $\langle 2\rangle$, as shown for $T>T_2$ in Fig. 3. [Note that this argument fails for $\bar{y}(1+y)$ too close to unity: there, $\tilde{W}_2(3)\to 0-$, so that the minimum of $\tilde{W}_2(l)$ may be at $l_{\max}=4$, thereby allowing $\langle 112\rangle$ to persist between $\langle 1\rangle$ and $\langle 12\rangle$ for $\bar{y}(1+y)\gtrsim 1$. Such an amendment is still consistent with the previous results, insofar as (4.23) predicts that the leading term of $\overline{W}_3(1,1)\to 0-$ as $\bar{y}(1+y)\to 1+$, whence correction terms could drive $\overline{W}_3(1,1)$ positive and so stabilize $\langle 112\rangle$ for $\bar{y}(1+y)\gtrsim 1$.]

So far, no new information has been gained, but certain of the previous results have been verified from this new point of view. It remains to locate $l_{\max}\geq 4$ for case (i), $\bar{y}(1+y)<1$, but that question is easily answered by examination of the limiting form of $\tilde{W}_2(l)$ as $T\to 0$ (or $y$, $\bar{y}\to 0$). By (4.30) this is

$$\begin{aligned}\tilde{W}_2(l)\approx&\frac{w_0}{\bar{y}(1+y)^{1/2}}(1-y\bar{y})^2[1+\bar{y}^2(1+y)][\tfrac{1}{2}q_1(1-y)\bar{y}(2+y)^{1/2}w_0]^{k+1}\\ &\times\sin\{\tfrac{1}{4}(k+1)[\pi+y+O(y^2)]+2\bar{y}(1+y)^{1/2}[1+O(\bar{y}^2)]\}\ ,\end{aligned} \tag{4.35}$$

with $l=k+2$. This implies $\tilde{W}_2(4)>0$ but $\tilde{W}_2(5)<0$ as $T\to 0$, whence $l_{\max}=k_{\max}+2=5$ in that limit. The arrangement of the simple periodic phases $\langle 1^k 2\rangle$ must therefore appear as shown in Fig. 3. At the very lowest temperatures, both $\langle 1^2 2\rangle$ and $\langle 1^3 2\rangle$ (and no others!) appear between $\langle 12\rangle$ and $\langle 1\rangle$. As $T$ increases, $\langle 1^3 2\rangle$ is cut off when $l_{\max}$ decreases from 5 to 4: this occurs approximately when $\tilde{W}_2(4)$ decreases through zero, and must, by continuity, be at a temperature $T_3(q_1)$ below that of the locus $\bar{y}(1+y)=1$ (at $T=T_2$) where $\tilde{W}_2(3)$ decreases through zero and $l_{\max}$ becomes 3.

In the phase diagram as developed from this point of view of 2-band walls separating $\langle 1\rangle$-phase domains, then, the $n$-wall interactions $\tilde{W}_n$ for $n\geq 3$ would be needed to resolve further only the three remaining pseudoboundaries $\langle 2\rangle$:$\langle 12\rangle$, $\langle 12\rangle$:$\langle 1^2 2\rangle$, and $\langle 1^2 2\rangle$:$\langle 1^3 2\rangle$.

(As explained at the beginning of Sec. V of part I of this series, the boundaries $\langle 1^k 2\rangle$:$\langle 1\rangle$ $(k=1,2,3)$ of the $\langle 1\rangle$ phase must all represent stable, first-order transitions and so need not be checked further for stability.) The $\langle 2\rangle$:$\langle 12\rangle$ pseudoboundary has of course already been resolved much further in Secs. IV A and IV B, so attention will be focused on $\langle 1^k 2\rangle$:$\langle 1^{k+1}2\rangle$ for $k=1,2$. Their stability is governed by $\tilde{W}_3(3,3)$ and $\tilde{W}_3(4,4)$, respectively. The appropriate transfer-matrix expression analogous to (3.12) is

$$\tilde{W}_3(k+2,k+2)=(\mathbf{c}_0^\dagger-\mathbf{b}_0^\dagger)\mathbf{C}^{k+1}\mathbf{B}\mathbf{C}^{k+1}(\mathbf{b}_1-\mathbf{c}_1)w_0^{2k+4}[1+O(w_0)]\ . \tag{4.36}$$

The form of $\tilde{W}_3(l,l)$ for arbitrary $\bar{y}\in(0,1)$ is algebraically messy and not of especial interest here, so we present only the leading terms for small $\bar{y}$, namely,

$$\tilde{W}_3(l,l)=\frac{w_0}{2\bar{y}^3(1+y)(2+y)^{1/2}}(1-y\bar{y})^2[\tfrac{1}{2}q_1(1-y)\bar{y}(2+y)^{1/2}w_0]^{2k+3}\{1+O(\bar{y}^2)-\cos[2(k+1)\Omega+O(\bar{y})]\}\ , \tag{4.37}$$

with $l=k+2$. From this it is clear that, at sufficiently low temperatures, both $\tilde{W}_3(3,3)$ and $\tilde{W}_3(4,4)$ are *positive,* whence both of the intermediate phases $\langle 12^12\rangle$ and $\langle 1^221^32\rangle$ must appear, as shown in Fig. 3. Their (pseudo)boundaries are decorated with dots, since they may be unstable to still further phases, although we have not performed the calculation of $\tilde{W}_n$ $(n\geq 4)$ necessary to address that question. In any case, it is clear that this brief discussion from the viewpoint of 2-band walls between $\langle 1\rangle$-phase domains has both confirmed some of the previous results, and helped further to elucidate the intricate arrangement of the many phases that are evidently present in the $CC_3$ model.

### D. Mean-field limit and higher-order corrections

All these results retain their validity with no significant changes in the limit $q_i\to\infty$ with $q_iJ_i$ constant $(i=0,1)$. In that limit, $y\to 1$, while $\bar{y}$ replaces $y$ as the axial Boltzmann factor. One has

$$\Delta(\bar{y})=2\bar{y}^2-1 \tag{4.38}$$

and, in (4.14) and (4.23) for $\overline{W}_2(l)$ and $\overline{W}_3(l,l)$, the replacement

$$\tfrac{1}{2}q_1(1-y)\to\tfrac{3}{4}q_1K_1\ . \tag{4.39}$$

No other changes are needed. Now this limit must correspond precisely to the mean-field limit of the $CC_3$ model, by analogy with the proof of Kac and Helfand[14] for the simple Ising model with "infinitely weak, infinite-range" pair interactions. One therefore reaches the conclusion that the low-temperature phase diagram of the *mean-field* $CC_3$ model (Fig. 3) differs qualitatively from that of the original $(q_1=2)$ model (Fig. 1 of Ref. 6). In particular, the mean-field phase diagram (the one most often studied by numerical calculations and simulations) will contain, arbitrarily close to the multiphase point, mixed phases and, possibly, even a complete devil's staircase, which are *not* present for the original simple-cubic-lattice model. Partial verification of these conclusions has been provided by some recent work of Siegert and Everts.[8] By calculating the leading terms of an exact low-temperature series expansion of the *mean-field* free energy of the $CC_3$ model, they demonstrated that the simplest of the mixed phases, $\langle 112\rangle$ (with mean wave vector $\bar{q}=2\pi/4$), persists all the way down to the multiphase point $\kappa=\frac{1}{2}$ at $T=0$. The examination of higher-order mixed phases $\langle 12^k12^{k+1}\rangle$ was not possible in the order to which they carried their expansion.[8]

Our discussion of the $CC_3$ model will be closed with a brief reconsideration of the effects of higher-order corrections. The remarks of Sec. III B apply equally well to the present case of arbitrary $q_1>2$, except that the splitting between the eigenvalues $\lambda_\pm$ is no longer $O(y)$ but rather $O(\Delta)$. One should therefore replace $y$ by $\Delta$ in (3.35) to obtain the conditions under which the contributions of out-of-chain spin flips (the leading source of error) are negligible. Notice that only a narrow range of values of $\Delta$ near 0, of width $O(w^{q_0-2})$, is affected.

A general analysis of the possible effects that may arises from these corrections has been presented in Sec. VII of part I, assuming that the enlarged transfer matrix **D** of (3.32) can be projected down to a $2\times 2$ matrix again. (See Sec. III E of part II for an example of a similar projection in the context of the ANNNI model.) For the general case, where the matrix **D** of (4.10) would acquire off-diagonal perturbation terms that do not vanish at $\Delta=0$, the range of behavior that can arise may be briefly summarized. At the simplest level, the location of the quasitricritical point may just be shifted slightly, to $\Delta=\Delta_0=O(w^{q_0-2})$, but it would continue to separate a case A regime at $\Delta<\Delta_0$ from a case B regime at $\Delta>\Delta_0$. (This is illustrated by a sample calculation below.) A more complex possibility, however, is that a new, narrow case A regime may appear wholly *within* the case B regime at $\Delta>\Delta_0$, whence an additional *pair* of quasitricritical points would be located at the ends of this new case A regime: this phenomenon has been analyzed in a general context in Sec. VII of part I.

In any event, only the stability of the highest-order $\langle 12^k\rangle$ phases in Fig. 3, near the $\langle 2\rangle$ boundary, would be affected. The low-order $\langle 12^k\rangle$ phases, governed by the form of the two-wall interaction $\overline{W}_2(l)$ at values of $l$ significantly less than the location $l_{\max}$ of any negative minimum it may have, cannot be destroyed by small shifts in the amplitude of $\overline{W}_2(l)$. Finally, note that one cannot, prior to actual calculation, rule out for the $CC_3$ model any of the possible effects just discussed, because

one does not expect the leading corrections to the transfer matrix **D** to exhibit any special symmetry. The matrix elements are indexed by the initial and final states of the flipped spins, hence the leading corrections, due to an extra out-of-chain spin flip, will probably affect all the matrix elements asymmetrically.

To illustrate one *possible* type of behavior in the crossover region about $\Delta=0$, consider the more easily investigated but less important effect of the nonzero value of the exponent $\theta$ in the matrices **B** and **C**. According to (4.7) and (4.8), the correction terms introduced into these matrices are $O(w_0)$, and hence become significant when

$$\Delta\equiv\tilde{y}^{\,2}(1+y)-1=\alpha w_0 \ , \tag{4.40}$$

with $\alpha$ of order unity. With $\Delta$ of this size, one has

$$\tilde{y}=1+O(y) \ , \tag{4.41}$$

whence $q_1=2+\delta q_1$ with $\delta q_1 \ll 1$. It is then a simple matter to substitute (4.7) and (4.8) into **B** and **C** as given by (4.3) and (4.4), and so conclude that the product matrix $\mathbf{D}\propto\mathbf{CB}$, as defined by (4.10), is modified to

$$\mathbf{D}=\begin{bmatrix} 1+\tilde{y}^{\,2} & \tilde{y}\Delta+6w_0 \\ \tilde{y}\Delta-6w_0 & 1+\tilde{y}^{\,2}+\Delta(2+\Delta) \end{bmatrix}+O(yw_0) \ . \tag{4.42}$$

The eigenvalues of **D** are now no longer given by (4.12) but rather by

$$\lambda_{\pm}=u(y)+O(yw_0)\pm w_0[2\alpha^2-36+O(y)]^{1/2} \ . \tag{4.43}$$

They therefore become *complex* within a crossover region defined by $|\alpha|<3\sqrt{2}+O(y)$; this leads to exponentially damped sinusoidal $n$-wall interactions $\overline{W}_n$, as indicated in Fig. 2(b), thus shifting the quasitricritical point to $\Delta\simeq 3\sqrt{2}w_0$. There would then be only finitely many $\langle 12^k\rangle$ phases between $\langle 1\rangle$ and $\langle 2\rangle$ at any fixed temperature within this crossover region, but, because $\overline{W}_n$ for $n\geq 3$ also oscillate in sign, the $\langle 12^k\rangle$:$\langle 12^{k+1}\rangle$ boundaries might be unstable to intermediate phases. (Such a scenario is in fact realized near the $T=0$ multiphase point in the ANNNI model, as discussed in II.)

## ACKNOWLEDGMENTS

We wish to thank Julia M. Yeomans for informative conversations and correspondence. The support of the National Science Foundation, in large part through the Materials Science Center at Cornell University but also through the Condensed Matter Theory Program,[15] is gratefully acknowledged.

---

*Present address: Department of Physics, University of Utah, Salt Lake City, UT 84112.

†Present address: Institute for Physical Science and Technology, University of Maryland, College Park, MD 20742.

[1]M. E. Fisher and A. M. Szpilka, Phys. Rev. B **36**, 644 (1987), herein denoted as part I.

[2]M. E. Fisher and A. M. Szpilka, preceding paper, Phys. Rev. B **36**, 5343 (1987), herein denoted as part II.

[3]S. Ostlund, Phys. Rev. B **24**, 398 (1981).

[4]D. A. Huse, Phys. Rev. B **24**, 5180 (1981).

[5]A. M. Szpilka and M. E. Fisher, Phys. Rev. Lett. **57**, 1044 (1986).

[6]J. M. Yeomans and M. E. Fisher, J. Phys. C **14**, L835 (1981).

[7]J. M. Yeomans and M. E. Fisher, Physica **127A**, 1 (1984).

[8]M. Siegert and H. U. Everts, Z. Phys. B **60**, 265 (1985); see also M. Siegert, Diplom-Arbeit, Universität Hannover, 1984.

[9]J. M. Yeomans, J. Phys. C **15**, 7305 (1982).

[10]J. M. Yeomans, J. Phys. C **17**, 3601 (1984).

[11]Note that $K_1$ in the notation of Yeomans and Fisher (Refs. 6 and 7) corresponds to $K_1\cos(2\pi/3)\kappa=\frac{1}{2}K_1[1+O(\delta)]$ in the notation used here.

[12]Note that our choice of signs in (2.18), and our convention for the standard structural coefficients, differ from that of Yeomans and Fisher (Ref. 7).

[13]Here, **D** is taken to be twice the matrix defined by Yeomans and Fisher (Ref. 7). This is more convenient for generalization to arbitrary $q_1$ in Sec. IV.

[14]M. Kac and E. Helfand, J. Math. Phys. **4**, 1078 (1963).

[15]Under Grant No. DMR 87-01223.